Design of a bilayer ceramic capacitor with low temperature coefficient of capacitance

P. Y. Foeller, J. S. Dean, I. M. Reaney, and D. C. Sinclair

Articles you may be interested in

Influence of temperature on the dielectric nonlinearity of BaTiO3-based multi-layer ceramic capacitors
Appl. Phys. Lett. **108**, 242902 (2016); 10.1063/1.4953626

Tuning of dielectric, pyroelectric and ferroelectric properties of 0.715Bi0.5Na0.5TiO3-0.065BaTiO3-0.22SrTiO3 ceramic by internal clamping
AIP Advances **5**, 087145 (2015); 10.1063/1.4929328

Ferroelectric phase transition and low-temperature structure fluctuations in Ba 4 Nd 2 Ti 4 Nb 6 O 30 tungsten bronze ceramics
J. Appl. Phys. **105**, 124110 (2009); 10.1063/1.3157147

(1 − x) Ba Ti O 3 − x (Na 0.5 K 0.5) Nb O 3 ceramics for multilayer ceramic capacitors
Appl. Phys. Lett. **90**, 132905 (2007); 10.1063/1.2717559

Dielectric behavior and microstructure of (Bi 1∕2 Na 1∕2) TiO 3 – (Bi 1∕2 K 1∕2) TiO 3 – BaTiO 3 lead-free piezoelectric ceramics
J. Appl. Phys. **97**, 104101 (2005); 10.1063/1.1890453

Design of a bilayer ceramic capacitor with low temperature coefficient of capacitance

P. Y. Foeller,[a] J. S. Dean, I. M. Reaney, and D. C. Sinclair

Functional Materials and Devices Group, Department of Materials Science and Engineering, University of Sheffield, Sheffield S1 3JD, United Kingdom

We show how a simple bilayer system that combines a layer of undoped $BaTiO_3$ (BT) with a second layer of $Ba_{0.975}Na_{0.025}Ti_{0.975}Nb_{0.025}O_3$ (2.5NNBT) can be used to improve the temperature coefficient of capacitance (TCC) of $BaTiO_3$-based materials for capacitor applications. The bilayer system emulates the volume ratio between a conventional core and shell phase microstructure allowing a simple resource efficient approach to optimise the system for low TCC. Optimisation was achieved with a volume ratio of 0.67 2.5NNBT with 0.33 BT and results in a TCC of $\pm 6\%$ over the temperature range ~25 to 125 °C whilst maintaining a permittivity of $\varepsilon_r \sim 3000$ and low dielectric loss. © 2016 Author(s). All article content, except where otherwise noted, is licensed under a Creative Commons Attribution (CC BY) license (http://creativecommons.org/licenses/by/4.0/). [http://dx.doi.org/10.1063/1.4961616]

Multi-layer ceramic capacitors (MLCC) are essential components for consumer electronics with their global market exceeding 2 trillion units per year.[1] High permittivity and good temperature stability are two of the main factors for the ceramic capacitor industry. $BaTiO_3$ (BT) is the current material of choice for dielectric layers due to its high permittivity, excellent dielectric properties, and the ability to extensively modify the Curie temperature, T_C at ~120–130 °C, by appropriate chemical doping of either or both of the cation sub-lattice sites. Its temperature dependent permittivity, referred to as the Temperature Coefficient of Capacitance (TCC), is modified with the use of such dopants[2,3] to achieve a TCC to meet industry standards, such as X7R ($\pm 15\%$ from −55 to 125 °C).[4]

Commonly used dopants for BT are intermediate sized rare-earth (RE) trivalent ions, such as Y and Dy being used for both Ba and Ti sites.[5–10] Limited diffusion of the dopants into BT grains leads to a concentration gradient of doped BT resulting in a "core-shell-like structure" (CS).[5,6,11–15] This structure can be considered to be a core-region of undoped BT ($Tc \sim 120$–130 °C) surrounded by a shell-region of micro volumes of different dopant concentrations, leading to a spread of Curie temperatures.[12] This approach engineers CS microstructures with a broad permittivity-temperature profile, reducing TCC to the levels required for industry standard ratings. Inducing a CS microstructure requires an iterative approach which is resource intensive. Recently, Maurya *et al.* adapted the concentration gradient of CS into a set of 70 layered doped compositions connected in either parallel or series.[16] The total capacitance of the series-type system was calculated using

$$\frac{1}{C_{total}} = V_{r1}\frac{1}{C_1} + V_{r2}\frac{1}{C_2}, \qquad (1)$$

where V_r is the volume ratio of a material, C is the capacitance of a material, and C_{total} is the total capacitance of the series-type system.

While this method has produced promising results, particularly for the series configuration, each layer is individually contacted to the electrodes. The overall permittivity will thus be dominated by the highest permittivity layer for the parallel set-up or the lowest permittivity layer for the series configuration (Fig. 1).

To minimise TCC in this arrangement, many layers are required. Thus, the shrinkage rate during ceramic processing is constrained, and as such the compositional variation that can be used is limited. Precise control of the interfacial coupling is key, and with ~70 different compositions, this design approach is unattractive from a commercial viewpoint.

We have recently reported the use of finite element modelling to predict the required optimal volume fraction of a CS structure to obtain minimisation of the TCC response based on a combination of two materials. Minimisation of TCC was obtained by using experimentally determined permittivity (ε)-T characteristics of undoped BT (core) and various compositions in a $NaNbO_3$-$BaTiO_3$ (NNBT) solid solution series (shell).[17] This led to the conclusion that combining 2.5NNBT with BT produced the most improved TCC
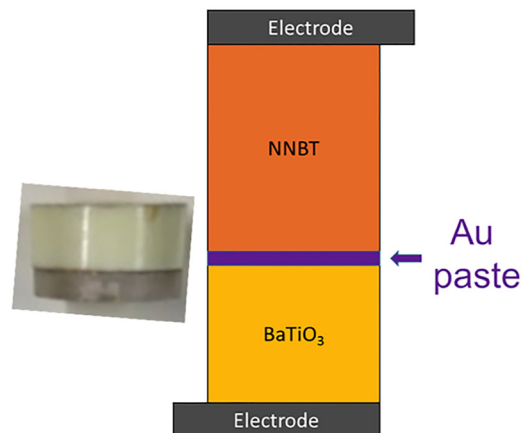
FIG. 1. Schematic and an example of a 2.5NNBT-BT bilayer ceramic in a series configuration.

[a] Author to whom correspondence should be addressed. Electronic mail: pyfoeller1@sheffield.ac.uk

109, 082904-1

characteristics. In contrast to the multi-composition approach of Maurya's, our design is based on only two compositions, one of which is undoped BT (Fig. 1). This methodology is therefore more attractive since it is based on viable, high throughput ceramic processing routes.

$x(NaNbO_3)$–$(1-x)BaTiO_3$ (2.5NNBT, $x = 0.025$) powder was prepared *via* a solid state reaction. $BaCO_3$ ($\geq 99\%$, Sigma-Aldrich, Dorset, UK), TiO_2 ($\geq 99.9\%$, rutile, Sigma-Aldrich, Dorset, UK), Na_2CO_3 ($\geq 99.5\%$, Fisher Scientific, Loughborough, UK), and Nb_2O_5 (99.999%, Stanford Materials Corporation, USA) were used in appropriate quantities to produce a ~ 50 g stoichiometric batch. Each reagent was weighed to an accuracy of ± 0.001 g and the resulting mixture was ball-milled in iso-propanol using 10 mm diameter Y_2O_3-stabilized Zr milling media for 12 h. After milling, the slurry was dried at 80 °C for 12 h.

The dried sample was sieved through a 250 μm mesh sieve and the resulting powder reacted in an alumina crucible at 1140 °C for 6 h. Following this, the powder was ball-milled, dried, and sieved again. Green pellets with a 10 mm diameter were pressed in a uniaxial press at ~ 0.3 tonne for ~ 1 min, then placed on Pt-foil in an alumina crucible, and sintered in air at 1400 °C for 8 h.

$BaTiO_3$ powder was obtained from an industrial source (AVX Ltd.) and pellets were pressed and sintered under the same conditions as 2.5NNBT. Lattice parameters for BT and 2.5NNBT from powder obtained from crushed sintered pellets were obtained by powder x-ray diffraction (XRD) using an X-ray diffractometer (PANalytical X'PERT[3], Almelo, The Netherlands). Pellet density was obtained using the Archimedes method (MS-DNY-43, Mettler Toledo). Ceramics were polished and coated with Au-paste, which was fired on at 800 °C. The dielectric properties of the individual pellets and then the combined bilayer, using various inner electrode arrangements (described later), were measured using an LCR meter (Agilent E4980 Precision LCR Meter, Agilent Technologies) with an applied ac voltage of 100 mV. Data points were collected every 60 s from room temperature (RT) to 150 °C using a non-inductively wound tube furnace at a rate of 1 °C min^{-1} and corrected for sample geometry. Thermal expansion of the materials was determined by a DIL 402 C (Netzsch, Selb, Germany) with a heating rate of 5 °C/min and a temperature range of 25 to 1400 °C. Scanning electron microscopy (SEM) was carried out on sintered pellets of 2.5 NNBT and BT. Pellets were initially polished with 800, 1200, and 2500 grit silicon carbide paper, followed by 6, 3, and 1 μm diamond polish pastes on synthetic polishing cloths. Following an acetone wash, they were thermally etched for 1 h at 90% of their sintering temperature. The etched pellets were mounted on aluminium stubs using silver paste (Agar Scientific Ltd., Stansted, UK) and coated with a conducting gold layer (EMSCOPE SC500A, Quorum Technologies, Laughton, UK). The samples were examined using an Inspect F50 FEG (FEI, Hillsboro, Oregon, USA) SEM operating at a spot size of 3.0 μm and 20 kV.

To optimise the TCC in the bilayer system, we alter the thickness of the individual layers. To control the thickness, the amount of each powder required for a specific fraction was pre-determined using the equation below

$$d = v_f \times \rho, \tag{2}$$

where d is the mass of dielectric material required for correct thickness, v_f the volume fraction of the dielectric material, and ρ the density of the ceramic after sintering at 1400 °C for 8 h. This amount was then adjusted to be as close to 1 g as feasible. The pellet dimensions were measured after polishing and before the application of electrodes to ensure the relative thicknesses were within $\pm 1\%$ of the desired volume fraction.

Ceramics were confirmed to be single-phase by XRD with lattice parameters, a = 3.9939(1) and c = 4.0375(1) Å for BT and a = 4.0027(1) and c = 4.0201(1) Å for 2.5 NNBT giving c/a ratios of 1.011 and 1.004 for BT and 2.5NNBT, respectively. BT has a higher shrinking onset temperature and finishes with a slightly smaller shrinkage compared to 2.5NNBT, Fig. 2(a). The sintering process results in dense ceramics, 98% for BT and 95% for 2.5NNBT as confirmed by SEM, Figs. 2(b) and 2(c). The bilayers were constructed from undoped BT and 2.5 NNBT ceramics. The pellets were not co-sintered for this work; however, the dilatometry performed on the individual materials suggests that co-sintering could be feasible, Fig. 2(a).

The permittivity versus temperature profiles for BT and 2.5 NNBT ceramics are shown in Fig. 3(a). BT has a room temperature (RT) permittivity of ~ 2500 which rises to a sharp maximum of ~ 7100 at 126 °C (Curie Temperature, T_C). In contrast, 2.5 NNBT has a RT permittivity of ~ 3900 and has a broad permittivity maximum of ~ 4800 at ~ 60 °C with evidence of a secondary broad peak of ~ 3500 at ~ 110 °C.
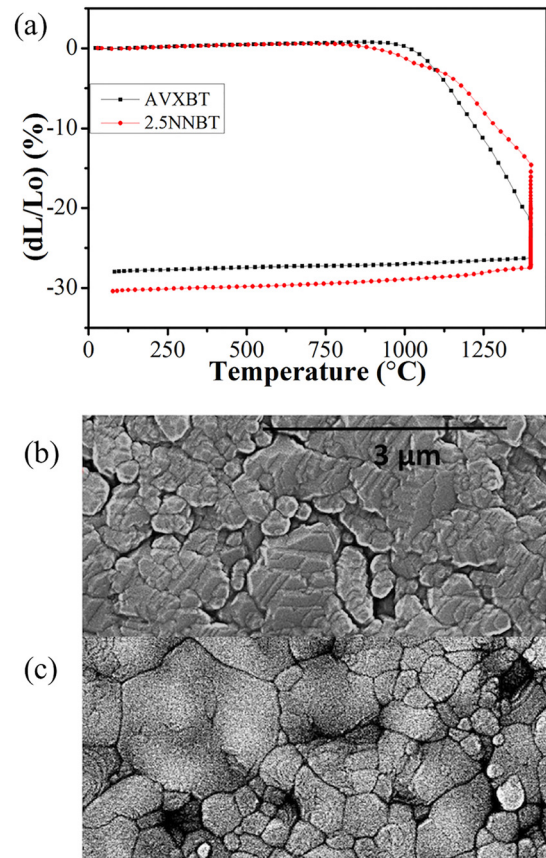
FIG. 2. (a) Dilatometer profiles of green pellets for the individual components of the bilayers and SEM micrographs of sintered (b) BT and (c) 2.5NNBT ceramics.
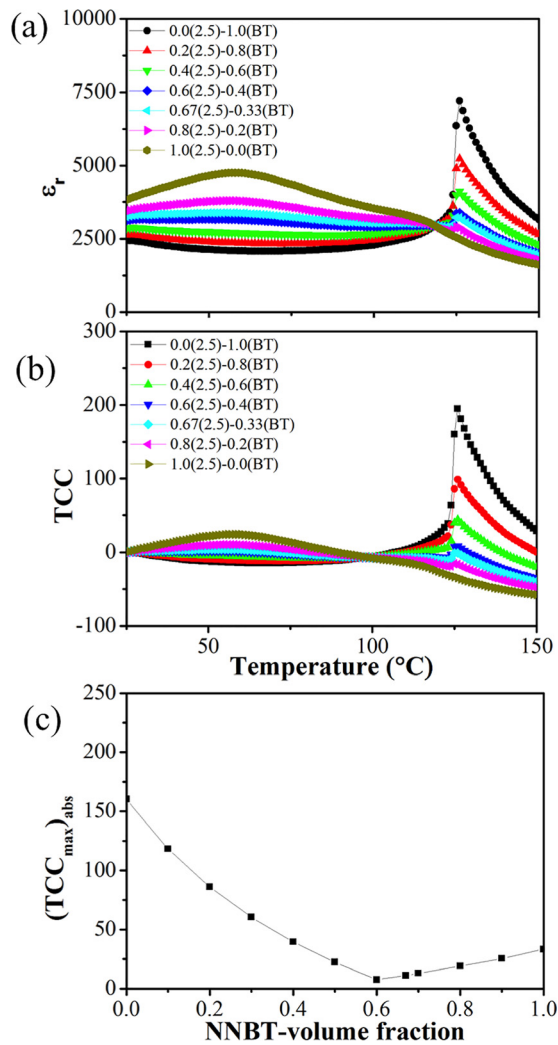
FIG. 3. (a) Experimentally measured permittivity-temperature profiles of BT (filled black symbols) and 2.5NNBT (filled olive green symbols) ceramics with simulated permittivity-temperature data from the series bilayer model for various volume fractions, v_f, e.g., 0.2(2.5)–0.8(BT) corresponds to $v_f = 0.2$ (2.5 NNBT) and $v_f = 0.8$ (BT). (b) Converted TCC values and (c) the maximum deviation of TCC versus v_f of 2.5 NNBT.

The corresponding TCC profiles were calculated using Equation (3), where

$$TCC = \frac{\Delta\varepsilon}{\varepsilon_{25}\Delta T}, \qquad (3)$$

the change in temperature ΔT is relative to 25 °C and $\Delta\varepsilon$ is the change in relative permittivity ε_r relative to the value obtained at 25 °C and denoted by ε_{25}.

The profiles in Fig. 3(a) show the large variation of TCC for BT which is initially negative but becomes strongly positive around T_C, whereas 2.5 NNBT shows much lower TCC that is initially positive but becomes strongly negative above $\sim$100 °C, Fig. 3(b).

These two permittivity-temperature profiles were used as input data sets for optimisation. They were connected in a series arrangement with various thicknesses, and hence volume fractions in an attempt to minimise TCC. The variations in permittivity and TCC for a two layer series-type system with various volume fractions of BT and 2.5 NNBT are shown in Figs. 3(a) and 3(b), respectively.

The simulations clearly show the strong suppression of the large permittivity and TCC of BT near T_C as the volume fraction of 2.5 NNBT increases in the series bilayer model. To simplify the optimisation, we employ a simple metric of the maximum deviation (absolute) of TCC from zero based on Fig. 3(b). The result of which is shown in Fig. 3(c). This can be used to estimate the optimised volume fraction of 2.5 NNBT and BT to obtain the lowest TCC. The results indicate that bilayers based on $v_f \sim 0.6$ to 0.7 of 2.5 NNBT achieve the lowest TCC values.

To verify the prediction from the model, ceramics based on $v_f = 0.67$ of 2.5 NNBT were prepared and connected in series as described in the experimental section. The permittivity and $\tan\delta$ profile of the bilayer are compared to those of its individual end member components in Fig. 4. This comparison shows the bilayer to have a permittivity of $\sim$3000 between 25 and 125 °C whilst retaining a low dielectric loss over the same temperature range. TCC of the bilayer compared to the end members is much improved, with TCC being as low as $\pm6\%$ over the temperature range of 25 to 125 °C.

Figure 4(a) does show a difference in the absolute permittivity of predicted combination and experimental data because the model assumes a perfectly flat interface between the two layers. Experimentally this is not the case as each layer is not perfectly flat and there is a layer of gold paste between the components (Fig. 5).

To confirm the effect(s) of interface roughness and possible incomplete electrode coverage, different interfaces were created to examine their influence on the permittivity values of the system. Pellets for a 60/40 2.5NNBT/BT bilayer were created and their permittivity collected with three kinds of interface between the pellets; Au foil, Au paste, and nothing
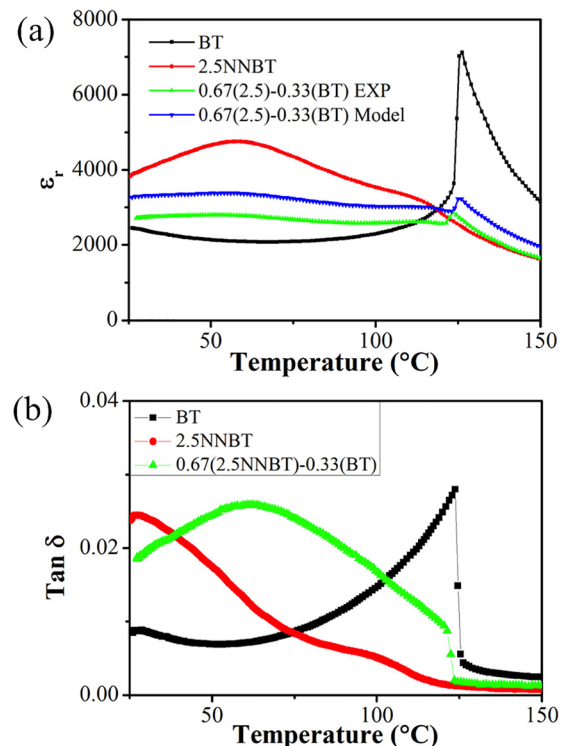
FIG. 4. (a) Permittivity and (b) $\tan\delta$ vs. temperature profiles for the 0.67/0.33 2.5NNBT/BT bilayer and its individual components.
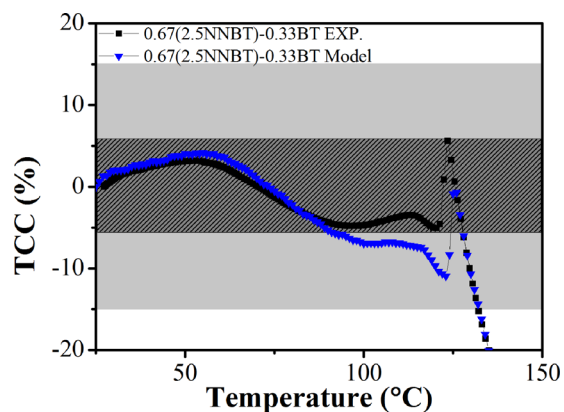
FIG. 5. A comparison of modelled and experimentally obtained TCC profiles for a bilayer BT-based ceramic based on $v_f = 0.67$ 2.5NNBT.

in-between the pellets. In the case of Au paste, two interfaces were fabricated. Au paste 1 interface was achieved by first coating the individual pellets with paste that was hardened and the pellets subsequently compressed together during measurements. Au paste 2 interface was achieved by a coat of paste between the two ceramics that was subsequently hardened to bond the two ceramics together. In the case of gold foil, a piece of gold was placed between the ceramics and the pellets subsequently compressed together during measurements. This arrangement was repeated twice (Au foil 1 and 2). The change in permittivity for the different interfaces is shown in Fig. 6. The permittivity drops significantly when there is no inner electrode or when the Au electrode interface is created from either Au foil or Au paste 2. This highlights the importance of the electrode interface in the performance of the device and the need to achieve good interfacial contact between the pellets to obtain a high permittivity bi-layer ceramic. The poor internal electrode contacts are due to a combination of incomplete (or no) electrode coverage and surface roughness at the interface between the ceramics.

Although it is not a focal point of this study, the choice of compatible internal electrodes with the bilayer materials for any MLCC application is an important consideration. In the case here, the choice of NNBT which contains Na (and in the absence of any other dopants) may restrict the choice of internal electrode materials to Ag/Pd and Pt based on air sintering as opposed to base metal electrodes such as Ni that require sintering under reducing conditions. Further
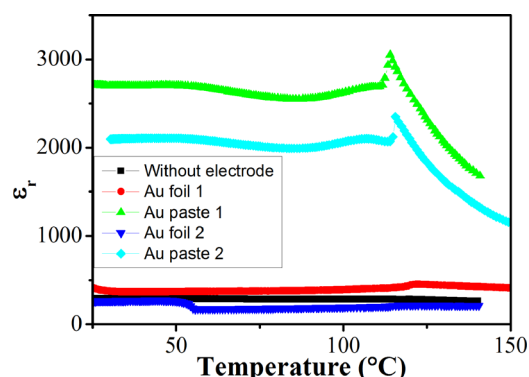
compatibility/processing studies are required to confirm this suggestion.

TCC has been successfully improved by creating a novel bilayer-system of 2.5NNBT and BT ceramics. The demonstrated methodology allows for optimisation of many different materials and the creation of a system with a permittivity of ~3000, low dielectric loss, and a TCC of ±6% over the range 25 to 125 °C, based on a volume ratio of 0.67 2.5NNBT to 0.33BT. Furthermore, it was shown that the interface between the layers exerts a significant influence on the permittivity, making it important to control the electrode interface between the ceramics. Further work is required as it is important to account for and potentially optimise the sub-ambient temperature region to achieve commercially popular specifications, e.g., X7R down to −55 °C, as well as to further understand the interface(s) between the ceramic layers.

[1]J. Ho, T. R. Jow, and S. Boggs, "Historical introduction to capacitor technology," IEEE Electr. Insul. Mag. **26**, 20–25 (2010).
[2]D. Hennings, A. Schnell, and G. Simon, "Diffuse ferroelectric phase transitions in Ba(Ti$_{1-y}$Zr$_y$)O$_3$ ceramics," J. Am. Ceram. Soc. **65**, 539–544 (1982).
[3]H. Kishi, Y. Mizuno, and H. Chazono, "Base-metal electrode-multilayer ceramic capacitors: Past, present and future perspectives," Jpn. J. Appl. Phys., Part 1 **42**, 1 (2003).
[4]See http://www.murata.com/~/media/webrenewal/support/library/catalog/products/capacitor/mlcc/c02e.ashx?la=en-us for Murata – Chip Monolithic Ceramic Capacitors.
[5]C.-H. Kim, K.-J. Park, Y.-J. Yoon, M.-H. Hong, J.-O. Hong, and K.-H. Hur, "Role of yttrium and magnesium in the formation of core–shell structure of BaTiO$_3$ grains in MLCC," J. Eur. Ceram. Soc. **28**, 1213–1219 (2008).
[6]C.-C. Chou, C.-S. Chen, I. N. Lin, W.-C. Yang, and H.-F. Cheng, "Development of X7R type base-metal-electroded BaTiO$_3$ capacitor materials by Co-doping of MgO/Y$_2$O$_3$ additives," Ferroelectrics **332**, 35–39 (2006).
[7]J. Nishikawa, T. Hagiwara, K. Kobayashi, Y. Mizuno, and H. Kishi, "Effects of microstructure on the Curie temperature in BaTiO$_3$-Ho$_2$O$_3$-MgO-SiO$_2$ system," Jpn. J. Appl. Phys., Part 1 **46**, 6999–7004 (2007).
[8]H. Kishi, N. Kohzu, J. Sugino, H. Ohsato, Y. Iguchi, and T. Okuda, "The effect of rare-earth (La, Sm, Dy, Ho and Er) and Mg on the microstructure in BaTiO$_3$," J. Eur. Ceram. Soc. **19**, 1043–1046 (1999).
[9]D. Makovec, Z. Samardzija, and M. Drofenik, "Solid solubility of holmium, yttrium, and dysprosium in BaTiO$_3$," J. Am. Ceram. Soc. **87**, 1324–1329 (2004).
[10]K.-J. Park, C.-H. Kim, Y.-J. Yoon, S.-M. Song, Y.-T. Kim, and K.-H. Hur, "Doping behaviors of dysprosium, yttrium and holmium in BaTiO$_3$ ceramics," J. Eur. Ceram. Soc. **29**, 1735–1741 (2009).
[11]Z. Tian, X. Wang, H. Gong, T.-H. Song, K. H. Hur, and L. Liz, "Core–shell structure in nanocrystalline modified BaTiO$_3$ dielectric ceramics prepared by different sintering methods," J. Am. Ceram. Soc. **94**, 973–977 (2011).
[12]C. A. Randall, S. F. Wang, D. Laubscher, J. P. Dougherty, and W. Huebner, "Structure property relationships in core-shell BaTiO$_3$-LiF ceramics," J. Mater. Res. **8**, 871–879 (1993).
[13]M. J. Pan and C. A. Randall, "A brief introduction to ceramic capacitors," IEEE Electr. Insul. Mag. **26**, 44–50 (2010).
[14]H. Y. Lu, J. S. Bow, and W. H. Deng, "Core–shell structures in ZrO$_2$-modified BaTiO$_3$ ceramic," J. Am. Ceram. Soc. **73**, 3562–3568 (1990).
[15]S.-C. Jeon, C.-S. Lee, and S.-J. L. Kang, "The mechanism of core/shell structure formation during sintering of BaTiO$_3$-based ceramics," J. Am. Ceram. Soc. **95**, 2435–2438 (2012).
[16]D. Maurya1, F.-C. Sun, S. P. Alpay, and S. Priya, "A new method for achieving enhanced dielectric response over a wide temperature range," Sci. Rep. **5**, 15144 (2015).
[17]J. S. Dean, P. Y. Foeller, I. M. Reaney, and D. C. Sinclair, "A resource efficient design strategy to optimise the temperature coefficient of capacitance of BaTiO$_3$-based ceramics using finite element modelling," J. Mater. Chem. A **4**, 6896–6901 (2016).

FIG. 6. Permittivity profiles for different interfaces between the ceramic layers.